Published in final edited form as:

Nature. 2018 December ; 564(7735): 258–262. doi:10.1038/s41586-018-0740-8.

Reward behavior is regulated by the strength of hippocampus-nucleus accumbens synapses

Tara A. LeGates[1], **Mark D. Kvarta**[1,2], **Jessica R. Tooley**[3], **T. Chase Francis**[4], **Mary Kay Lobo**[4], **Meaghan C. Creed**[3], and **Scott M. Thompson**[1,2]

[1]Departments of Physiology,University of Maryland School of Medicine, Baltimore, MD

[2]Departments of Psychiatry,University of Maryland School of Medicine, Baltimore, MD

[3]Departments of Pharmacology, University of Maryland School of Medicine, Baltimore, MD

[4]Departments of Anatomy & Neurobiology, University of Maryland School of Medicine, Baltimore, MD

Reward drives motivated behaviors and is key for survival, resulting in strong evolutionary pressure to retain contextual information regarding rewarding stimuli. This drive may be abnormally strong, such as in addiction, or weak, such as in depression, in which anhedonia, or loss of pleasure to rewarding stimuli, is a prominent symptom. Hippocampal input to the shell of the nucleus accumbens (NAc) is important for driving NAc activity[1,2] and activity-dependent modulation of its strength may play a role in the proper regulation of goal-directed behaviors. However, there are few robust descriptions of the mechanisms underlying induction or expression of long-term potentiation (LTP) at these synapses and no evidence whether such plasticity contributes to reward-related behavior. Here, we demonstrate that high frequency activity induces LTP at hippocampus-NAc synapses via canonical, but dopamine-independent, mechanisms. The induction of LTP of this synapse *in vivo* drives conditioned place preference (CPP), and activity is required for CPP in response to a natural reward. Conversely, chronic stress, which induces anhedonia, decreases the strength of this synapse and impairs LTP, whereas antidepressant treatment is accompanied by a reversal of these stress-induced changes. We conclude that hippocampal-NAc synapses display activity-dependent plasticity and suggest that their strength may be critical for contextual reward behavior.

Correspondence to Scott Thompson (sthompson@som.umaryland.edu). Editorial Correspondence: Dr. Scott M. Thompson, Ph. D., Professor and Chair, Department of Physiology, University of Maryland, School of Medicine, 655 West Baltimore St., Baltimore, MD 21201, tel: (410) 706-5817, fax: (410) 706-8341.

Author Contributions

T.A.L, M.D.K, T.C.F., M.K.L., and S.M.T designed experiments. T.A.L performed viral injections and collected and analyzed behavior and whole-cell electrophysiological data. M.D.K collected data for behavior experiments and collected and analyzed c-Fos data. J.R.T. and M.C.C. collected and analyzed *in vivo* electrophysiology data. T.C.F. performed viral injections and collected behavior data. T.A.L and S.M.T drafted the article. M.D.K, T.C.F., M.K.L., and M.C.C. provided critical revisions. All authors approved of the final version.

The authors report no competing financial interest.

Data sets are available from the corresponding author upon request.

Hippocampal activity is altered by changes in contextual features of rewarding stimuli[3,4], and a population of reward associated cells have been identified in this region[5]. Activity-dependent enhancement of spike firing has been observed at hippocampus-NAc synapses[5,6], and cocaine strengthens connectivity between the two nuclei[6], leading us to hypothesize that plasticity of these excitatory synapses is associated with reward. We first examined whether hippocampus-NAc inputs display activity-dependent synaptic potentiation. Using whole-cell voltage-clamp, we recorded excitatory postsynaptic currents (EPSCs) from MSNs in the ventromedial NAc shell in brain slices from mice expressing td-Tomato in dopamine type 1 receptor (D1R)-expressing MSNs to differentiate D1R- and presumptive D2R-expressing cells[7]. Glutamatergic EPSCs, mediated by both α-amino-3-hydroxy-5-methyl-4-isoxazolepropionic acid (AMPA)- and *N*-methyl-D-aspartate (NMDA)-type receptors, were evoked by electrical stimulation of axons of hippocampal cells projecting to the NAc via the fornix. In response to high frequency stimulation (HFS) (Fig. 1a-c), robust potentiation was elicited similarly in both D1R- and D2R MSNs. LTP was accompanied by a change in coefficient of variation and reduction in transmission failures (Extended Data Fig. 1), but no change in paired-pulse ratio (Fig. 1a), suggesting post-synaptic expression mechanisms underlie this potentiation (Fig. 1a-c, Extended Data Fig. 1).

To verify that fornix-evoked EPSCs were produced by hippocampal input to the NAc, we recorded photostimulation-evoked EPSCs (pEPSCs) in slices from mice expressing channelrhodopsin (ChR) in ventral hippocampus (vHipp) pyramidal neurons (Extended Data Fig. 2). Light pulses delivered in the NAc evoked pEPSCs comparable to EPSCs elicited by electrical stimulation of the fornix. High frequency photostimulation (pHFS) elicited LTP of a similar magnitude and time course to that elicited by electrical HFS in the fornix (Fig. 1D-F). Furthermore, pHFS potentiated simultaneously recorded EPSCs and pEPSCs, evoked with alternating stimuli (Fig. 1g-i).

We next used pharmacological manipulation to dissect the mechanisms underlying hippocampus-NAc LTP. HFS did not induce LTP in MSNs in the presence of the NMDAR antagonist, 2-amino-5-phosphonovaleric acid (APV), whereas LTP was induced normally in slices in which APV was washed out prior to HFS (Fig. 1j-l). Loading the calcium chelator BAPTA into the cell also blocked induction of LTP, indicating that this is a Ca^{2+}-dependent process (Fig. 1j-l). In accordance, LTP induction was blocked by pretreatment of slices with a Ca^{2+}/calmodulin-dependent kinase type II (CaMKII) inhibitor, KN62 (Fig. 1j-l). These properties were observed in both D1R- and D2R-MSNs. Therefore, induction of LTP at hippocampal-NAc synapses requires NMDAR activation, elevation of intracellular [Ca^{2+}], and CaMK activation, much like canonical Schaffer collateral-CA1 cell LTP[8].

An essential mechanism for postsynaptic LTP expression is the insertion of AMPARs. In the ventral tegmental area, Ca^{2+} permeable AMPARs lacking GluA2 subunits are preferentially inserted during the expression of cocaine-induced plasticity[9,10]. We asked whether LTP induction altered subunit composition at hippocampus-NAc synapses. Prior to HFS, hippocampus-NAc EPSCs displayed a linear relationship between current and holding potential with no change in EPSC amplitude upon application of the selective inhibitor of GluA2-lacking AMPARs, *N*-acetyl-spermine (NASPM) (Extended Data Fig. 3), consistent with the presence of mostly Ca^{2+} impermeable, GluA2-containing AMPARs at the

synapse[10]. Following the induction of LTP, current-voltage relationships remained linear, and EPSCs remained insensitive to NASPM, suggesting that expression of LTP at hippocampus-NAc synapses does not involve insertion of GluA2-lacking AMPARs (Extended Data Fig. 3).

Dopamine is a critical neuromodulator in the NAc, and there is evidence that dopamine signaling is required for LTP induction in the NAc [10–14]. We recapitulated these findings using local stimulation to activate unidentified excitatory synapses within the NAc and found that LTP was blocked in the presence of the D1R antagonist, SCH 23390 (Extended Data Fig. 4). To examine the requirement of dopamine signaling for LTP specifically at hippocampus-NAc synapses, we recorded from D1R- and D2R-MSNs in the presence of their respective receptor antagonists, SCH 23390 and sulpiride. Robust LTP was elicited, suggesting that dopamine signaling is not required for the induction of LTP at this synapse in either cell type (Fig. 1m-o; Extended Data Fig. 5). We also examined signaling downstream of dopamine receptors by blocking PKA with Rp-cAMPs, which had no effect on the ability to elicit LTP in D1R-MSNs (Fig. 1m-o). Taken together, these data show that LTP at hippocampal-NAc synapses involves canonical NMDA receptor-dependent mechanisms but does not require dopamine signaling.

To determine a functional role for potentiation at hippocampus-NAc synapses *in vivo*, we tested whether LTP modulated reward measured by CPP. ChR2 or eYFP were expressed in vHipp. Because collaterals of NAc-projecting hippocampal cells were observed within the prefrontal cortex and amygdala (Extended Data Fig. 6), fibers were implanted into the NAc bilaterally to stimulate the hippocampus-NAc synapses selectively. Conditioning ChR-expressing mice with pHFS resulted in preference for the light-conditioned chamber, without altering locomotor activity (Fig. 2a-b; Extended Data Fig. 7). eYFP-expressing mice showed no preference for either chamber (Fig. 2a-b). 4Hz stimulation, which does not induce LTP in slices (Extended Data Fig. 8) did not induce CPP (Fig. 2c-d), suggesting that CPP was specifically dependent upon LTP induction.

To demonstrate LTP *in vivo,* we recorded light-evoked local field potentials (LFPs) in the NAc shell in mice expressing ChR2 in vHipp. We found that HFS induced LTP of light-evoked LFPs (Fig. 2e-g), similar to our whole-cell results. In contrast, LTP was not observed in response to 4Hz or under conditions where no stimulation paradigm was used (Fig. 2e-g). We also examined optogenetically-induced c-Fos expression as a marker of neuronal activation. HFS, but not 4 Hz, produced a robust increase in the number of c-Fos+ cells within the NAc shell, but not core (Extended Data Fig. 9), corresponding to the observed LFP potentiation. We conclude that HFS induces LTP at hippocampus-NAc synapses *in vivo*, presumably underlying the formation of CPP.

We then tested the contribution of this synapse to responses to natural rewards. Mice expressing the light-activated chloride pump, halorhodopsin (NpHR), or YFP in the vHipp were tested for CPP in response to social interaction. Light was delivered to the NAc during conditioning to silence activity at hippocampal inputs selectively. YFP-expressing mice displayed a preference for the chamber in which they had previously encountered the target animal, whereas NpHR-expressing mice did not, suggesting that activity of hippocampus-

NAc synapses during conditioning is critical for CPP (Fig. 2h-i). In contrast, silencing of hippocampus-NAc synapses did not interfere with the rewarding quality of the social interaction itself. Both NpHR- and YFP-expressing mice showed normal social interaction during light-induced synaptic silencing (Fig. 2j). This suggests that activity at this synapse is not necessary for generalized reward processing, but is necessary for encoding reward associated with spatial context.

Maintaining excitatory drive in the NAc is crucial for normal hedonic state[15,16]. Synaptic weakening in the NAc contributes to stress-induced anhedonia[15], although the source of the input was not identified. We predicted that chronic stress would decrease strength at hippocampus-NAc synapses. We used chronic multimodal stress (CMS) to induce anhedonic-like behavior, assayed by loss of sucrose preference (Fig. 3a). D1R-MSNs recorded in brain slices taken from mice with a loss of sucrose preference displayed a decrease in synaptic strength, as measured by a decrease in the ratio of AMPAR- to NMDAR-dependent components of the EPSC (AMPA:NMDA ratio) (Fig. 3b-c). This is consistent with previous descriptions of stress-induced AMPAR internalization[15]. Furthermore, induction of LTP was profoundly impaired in D1R-MSNs (Fig. 3d-e). In contrast, AMPA:NMDA ratios and LTP were unaltered by chronic stress in D2R-MSNs (Fig. 3b,c,e-g). D2R-MSNs instead displayed inward rectification at positive membrane potentials and sensitivity to NASPM (Extended Data Fig. 10), unlike D2R-MSNs in unstressed control mice, suggesting a stress-induced increase in the contribution of Ca^{2+} permeable, GluA2-lacking synaptic AMPARs. These data demonstrate that chronic stress selectively weakens the strength and impairs plasticity of hippocampal input to D1R-MSNs. Because activity of D1R-MSNs is associated with positive reward[17–20], these results suggest that the chronic weakening of excitatory drive of the NAc is a contributing factor in stress-induced anhedonia.

Since potentiation of the hippocampus-NAc synapse elicits CPP, while weakening was associated with anhedonia, we sought to determine the functional consequence of these stress-induced synaptic plasticity deficits. We observed that the ability of pHFS to induce CPP was abolished after exposure to chronic stress, in contrast to results prior to stress, in which pHFS induced CPP (Fig. 3h). This suggests that chronic stress interferes with CPP by weakening and impairing LTP at hippocampal synapses onto D1R-MSNs.

If dysfunction of hippocampus-NAc synapses contributes to stress-induced changes in reward behavior, then antidepressant treatment should restore normal reward behavior and reverse these synaptic changes. We treated mice that displayed loss of sucrose preference after CMS with the selective serotonin reuptake inhibitor, fluoxetine. Chronic fluoxetine treatment reversed loss of sucrose preference (Fig. 4a) and restored the CPP deficit induced by chronic stress (Fig. 4b). AMPA:NMDA ratios and LTP in D1R-MSNs from stressed mice treated with chronic fluoxetine were similar to those observed in unstressed controls (Fig. 4c-g). Similarly, stress-induced changes in AMPAR subunit composition observed in D2R-MSNs were restored after chronic fluoxetine treatment (Extended Data Fig. 10). Acute treatment (24–48 hours) with fluoxetine, which was not sufficient to restore normal sucrose preference, failed to reverse the chronic stress-induced synaptic changes in D1R-MSNs (Figs 4a,c-g). Taken together, these data suggest that restoration of excitatory synaptic

strength and plasticity at the hippocampus-NAc synapse coincides with the reinstatement of normal reward behavior.

Reward drives goal-directed behaviors and various aspects of this process, such as motivation, anticipation, and contextual information are encoded in different brain regions. We found that synapses formed by hippocampal inputs to the NAc are highly plastic. Brief correlated high frequency activity was sufficient to induce both long-term potentiation and a persistent contextual reward behavior. Recent work has also shown strengthening of hippocampus-NAc coupling in conjunction with cocaine-induced CPP[6]. The correlation between excitatory strength at this synapse and reward was reinforced by our observation that chronic stress induced deficits in reward related behavior, namely anhedonia, as well as weakening of excitatory synaptic strength and impairment of their plasticity. Conversely, restoration of strength and plasticity at this synapse in response to antidepressant treatment was accompanied by restoration of normal hedonic state. The plasticity of these synapses represents a novel mechanism in the biology of reward. Targeting reward circuits for further study will expand our understanding of the pathophysiology underlying depression and mechanisms of antidepressant response.

Methods

Animals.

Male Drd1a-tdTomato hemizygous mice were generated by mating a Drd1a-tdTomato hemizygous mouse to a C57BL/6 mouse and were used to differentiate D1R- and D2R-expressing MSNs. D1-expressing MSNs were identified by expression of tdTomato whereas unlabeled cells were presumed to be D2-expressing MSNs. All mice were used between 2–4 months of age. Mice were group housed in a 12:12 light/dark cycle with food and water ad libitum. All experiments were performed in accordance with the regulations set forth by the University of Maryland Institutional Animal Care and Use Committee.

Chronic Multimodal Stress.

Sucrose preference was assessed prior to starting CMS. Only mice that showed a sucrose preference (>70%) were used. Mice were confined to a restraint tube (IBI Scientific, Peosta, IA) in the presence of white noise and a strobe light for 4 hours per day, after which they were returned to their home cage and were individually housed. Mice were stressed daily for 10–14 days, and the procedure began no later than zeitgeber time ZT4 each day. Loss of sucrose preference (<65%) was used to assess stress susceptibility and defined a depression-like anhedonic state.

Sucrose Preference Test.

Mice were trained by introducing two bottles containing 2% sucrose to their home cage at least one full day prior to their initial testing. To assess sucrose preference, one bottle containing 1% sucrose in water and one bottle containing plain water were introduced at the beginning of the active (dark) phase. The bottles were removed at the end of the active phase and weighed to measure amount consumed. Sucrose preference was calculated by dividing

the volume of sucrose solution consumed by the total volume consumed (water and sucrose) and expressed as a percentage.

Antidepressant Treatment.

Mice with a sucrose preference (>70%) were subjected to CMS as described above. Upon loss of sucrose preference (<65%), mice were treated with fluoxetine (18 mg/kg/day) in their drinking water acutely (3 days) or chronically (3 weeks). Sucrose preference was tested following fluoxetine treatment.

Electrophysiology.

Standard methods were used to prepare 400μm parasagittal sections that contained both the NAc shell and the fornix, the source of NAc-projecting hippocampal efferents. Dissection and recording were performed in cold artificial cerebrospinal fluid (ACSF) containing (in mM) 120 NaCl, 3 KCl, 1.0 NaH_2PO_4, 1.5 $MgSO_4 \cdot 7H_2O$, 2.5 $CaCl_2$, 25 $NaHCO_3$, and 20 glucose and bubbled with carbogen (95% O_2-5% CO_2). Slices recovered for one hour and were then transferred to a submersion-type recording chamber and superfused at 20–22°C (flow rate 0.5–1 ml/min).

Cells were visualized under differential interference contrast using a 60× water immersion objective (Nikon Eclipse E600FN). D1 and D2-MSNs were identified by the presence or absence of tdTomato, respectively.

Whole-cell currents were recorded in the ventromedial region of the NAc shell under voltage-clamp conditions (−70mV) using an Axopatch 200B amplifier (Axon Instruments, Union City, CA) and digitized with a Digidata 1440 analog-digital converter (Instrutech, Elmont, NY). EPSCs were evoked electrically, by placing a bipolar stimulating electrode (FHC Bowdoin, ME) in the fornix, or optogenetically, by placing a fiber emitting 473nm blue light from a 473 nm diode-pumped solid-state laser (OEM Laser Systems Midvale, Utah) above the slice over the NAc shell. EPSCs were evoked at a frequency of 0.1Hz. Patch pipettes were pulled to resistances of 3–8MΩ. For LTP and mEPSC experiments, patch pipettes were filled with a solution containing 130mM K-gluconate, 5mM KCl, 2mM $MgCl_6$-H2O, 10mM HEPES, 4 mM Mg-ATP, 0.3mM Na_2-GTP, 10mM Na_2-phosphocreatine, and 1mM EGTA. For rectification and AMPA:NMDA ratio experiments, patch pipettes were filled with 135mM CsCl, 2mM $MgCl_6$-H_2O, 10mM HEPES, 4 mM Mg-ATP, 0.3mM Na_2-GTP, 10mM Na_2-phosphocreatine, 1mM EGTA, 5mM QX-314, and 100μM spermine. The extracellular solution consisted of ASCF and 50μM picrotoxin. For experiments involving pharmacological manipulation of signaling pathways involved with LTP induction (APV (Sigma 50μM), KN-62 (Tocris 3μM), Rp-cAMP (Tocris 5μM), SCH23390 (Tocris 3μM), Sulpiride (Tocris 10μM)), drugs were superfused over the slice for at least 15 minutes, after which baseline EPSCs were recorded and HFS was used to elicit LTP. To examine the requirement of Ca^{2+} signaling in LTP induction, BAPTA (Molecular Probes 10mM) was included in the patch pipette to block intracellular Ca^{2+}. To examine subunit composition changes after LTP induction, HFS was used to induce potentiation, and NASPM (Tocris 200μM) was applied after stable potentiated responses were recorded for 10 minutes. Recordings were discarded if access resistance changed by >20%.

Summary LTP graphs were generated by averaging the peak amplitudes of individual EPSCs in 5-min bins (six consecutive sweeps) and normalizing these to the mean value of EPSCs collected during the 10-min baseline immediately before the LTP-induction protocol (four bouts of 100Hz stimulation for 1s with 15s between bouts while holding the cell at −40mV). Individual experiments were then averaged together for graphical representation. The last five minutes of recording were used for statistical comparisons. For AMPA:NMDA ratios, the peak amplitude at −70 was used to quantify the AMPA component while the amplitude at +40mV at 50ms after stimulation (>3 time constants of the decay of AMPAR-mediated synaptic currents) was used to quantify the NMDA component. The investigator was blind to treatment groups during recording and analysis.

Virus and Optogenetic Fiber Placement Surgery.

Mice were anesthetized with 3% isoflurane and underwent stereotaxic surgery to inject serotype 5 adeno-associated viruses (AAV) containing CaMKIIa-ChR2(H134R)-eYFP, CAMKIIa-eNpHR3.0-YFP, or CaMKIIa-eYFP (UNC Viral Vector Core, Chapel Hill, North Carolina) and implant optic fibers. Virus was injected bilaterally into the vHipp (from bregma anterior/posterior: −3.7, lateral: +3.0, dorsal/ventral: −4.8 from top of skull) and was infused at a rate of 0.1 mL per minute. The injection needle was left in place for 10 minutes following the infusion. Mice recovered for 6–8 weeks to allow for infection of the hippocampal projections to occur. For *in vivo* optogenetic experiments, 4 mm chronically implantable fibers (0.22 numerical aperture, 105 micrometer core) were placed bilaterally to target the NAc (anterior/posterior: +1.6, lateral: +1.5, dorsal/ventral: −4.4 from top of skull).

Conditioned Place Preference (CPP).

Mice were allowed to recover from surgery for at least two weeks prior to behavior experiments. The ability of optogenetic potentiation to induce CPP was evaluated using a three chamber CPP arena (Maze Engineers), which consisted of two chambers distinguishable by visual cues and a smaller chamber connecting the two rooms. Behavior was monitored by a camera positioned above the arena, and data were collected using Anymaze software (Stoelting Co.). Mice were allowed to freely explore the entire arena for 30 minutes. During this habituation phase, mice were connected to a patch cord but no light was transmitted. Mice that showed an inherent preference >65% for either side of the arena were removed from the experiment. The following day, mice were connected to the patch cord and confined to one compartment during which they were conditioned with ~5mW 473nm light administered at four bouts of 100Hz stimulation for 1s (2ms pulse width) with 15s between bouts using a 473 nm diode-pumped solid-state laser (OEM Laser Systems Midvale, Utah). The mice remained in the arena for 30 minutes after stimulation. In a second session on the same day (~4 hours later), mice were confined to the other side of the arena while connected to a patch cord with no light administered. Whether mice received light or no light first was randomized. This was repeated and counterbalanced on following day. Following two days of conditioning, CPP was tested by allowing mice to freely explore the entire arena for 20 minutes. The experiment was performed similarly for CPP in response to 4Hz stimulation except mice were conditioned to light administered at four bouts of 4Hz stimulation for 25s with 15s between bouts.

For the experiments testing the effect of chronic stress and fluoxetine treatment on CPP, mice were subjected to stress, fluoxetine treatment, and CPP as described above. Sucrose preference and CPP were tested in all mice prior to stress. Mice were then exposed to chronic stress, and once sucrose preference was lost, mice underwent the CPP protocol again. Following this, mice were treated with fluoxetine and restoration of sucrose preference was measured followed by CPP. A separate group of mice continued to undergo stress but were not treated with fluoxetine. The experimenter was blinded to the groups during testing and analysis.

For experiments testing the effect of synaptic silencing, social interaction was used to induce CPP. Set up and habituation were performed as described above. The following day, mice were connected to the patch cord and confined to one compartment in the presence of a female mouse (target animal) while ~9–10 mW 473nm light was delivered (3s on/3s off) for 30 minutes. The target mouse was confined in a small wire cage to permit interaction. In a second session on the same day (~4 hours later), mice were confined to the other side of the arena while connected to a patch cord with no light administered and in the absence of a target animal. Whether mice received light or no light first was randomized. This was repeated and counterbalanced each day. Following three days of conditioning, CPP was tested by allowing mice to freely explore the entire arena for 20 minutes.

Social Interaction.

Social interaction was evaluated in a 33.65cm x 33.65cm arena with a 9.5cm diameter x 10cm height wire cage positioned on one side to hold the target animal. Behavior was monitored by a camera positioned above the arena, and data were collected using Anymaze software (Stoelting Co.). Mice were connected to a patch cord to deliver light (~9–10 mW, 473nm, 3s on/3s off) and placed on the side of the arena opposite the target cage in the absence of a target animal. Mice were allowed to freely explore for 150s after which they were returned to their home cages briefly while a target animal was placed in the target cage. Mice were then placed back into the arena opposite the target cage and allowed to explore for 150s. The time spent interacting with the target animal as defined by entry into the area immediately surrounding the target cage.

In vivo Electrophysiology.

CaMKIIa-ChR2(H134R)-eYFP (UNC) was injected into the vHipp as described above and an optic fiber (Thorlabs) was implanted over the vHipp and craniotomy was made over the NAc (from bregma in mm: +1.6 AP, +0.6 ML). A 16-channel, silicone recording probe (A1×16-Poly2–5mm-50s-177-A16, NeuroNexus, Ann Arbor) was lowered at a rate of 100 μm/sec to a depth of −4.5 mm to target the NAc shell. After allowing 20 min for the recording to stabilize, 10 msec light pulses (473 nm wavelength, Plexbright LED) were delivered through the optic fiber at 2.5 sec intervals. After a 10 min baseline recording, 4 stimulation trains (either 100 Hz or 4 Hz, 4ms pulse width, 15 second ISI) were applied through the optic fiber as described for slice physiology experiments, before resuming recording conditions identical to baseline for an additional 40 min. A mock stimulation group was included as a control (after 10 minutes of baseline recording, light pulses were stopped for 2 minutes before proceeding with recordings). After termination of the

recording, the silicone probe was removed, mice were sutured and returned to their home cage. Each mouse was recorded on each hemisphere for 2 recording conditions, the order of hemisphere and stimulation protocol was counter-balanced across subjects. Light evoked-responses in the local field potential (LFP) were analyzed using Neuroexplorer software (Plexon Inc, Austin, TX). Peri-event histograms of LFP responses were averaged for 24 trials (to yield 1 minute intervals) and then computed with 40 msec bins around onset of light stimulation. The difference between the LFP amplitude in the 40 msec bin immediately preceding light onset and peak LFP deflection was calculated for each 1-minute interval and was then plotted as a function of time. Only channels with significant light-evoked changes in the LFP response (as determined by repeated t-test during baseline recordings) were used in the analysis.

HFS induced c-Fos expression.

ChR-expressing mice were connected to patch cords while in their home cage, and 100Hz or 4Hz blue light was administered as described above. 100Hz stimulation was administered to YFP-expressing mice. Approximately 70 minutes later, mice were anesthetized with isofluorane. Once anesthetized, the mice were perfused transcardially with 0.9% saline followed by 4% paraformaldehyde. Brains were removed, postfixed overnight in 4% paraformaldehyde, and then transferred to 0.1M phosphate buffer (PB). Brains were sectioned (40μm) through the rostro-caudal extent of the NAc using a vibratome. Sections were stored free-floating in 0.1M PB. Sections were incubated in blocking buffer (0.1M PB, 3% triton X-100, 0.5% goat serum) for 2 hours. Sections were incubated in rabbit anti-c-Fos (Santa Cruz sc-52; 1: 1,000) overnight at 4°C and then visualized with a goat anti-rabbit fluorescent secondary antibody (Alexafluor 546). Sections were mounted on microscope slides and coverslipped with Vectashield. Slides were viewed and imaged on a Nikon Eclipse E400. Photoshop was used to count c-Fos positive cells and measure the area of region counted from. The number of c-Fos positive cells was normalized to the area of the region. The investigator was blinded to the groups during processing of tissue and cell counting.

Hippocampus-NAc projection labeling.

A retrograde virus expressing Cre recombinase (AAV5-hSyn-Cre-hGH; Penn Vector Core) was injected into the NAc shell (from bregma: anterior/posterior: +1.6, lateral : +0.6, dorsal/ventral: 4.5), and a Cre-dependent virus (AAV2-DIO-ChR2eYFP) was injected in the vHipp (from bregma anterior/posterior: −3.7, lateral: +3.0, dorsal/ventral: −4.8 from top of skull). Viruses were expressed for approximately 8 weeks to allow for labeling of hippocampal cells as well as their projections in the brain. Mice were then perfused as described above and brain postfixed as described above. 100μm sections were made through the rostral/caudal extent of the brain using a vibratome. Sections were mounted and coverslipped with Vectashield. 10× images were taken using a W-1 spinning disk confocal microscope (Nikon), and z-stacks were taken at 100× on a LSM 710 NLO (Zeiss). Maximum intensity projections of the z-stacks were generated in Image-J.

Statistical Analyses and Data.

Statistical analysis was performed using Graphpad Prism 6 software. When results are compared before and after HFS, n represents the number of cells or units. For all other experiments, n represents the number of mice. For electrophysiological experiments, this represents multiple cells recorded and averaged from each mouse. For box plots, the line in the middle of the box is plotted at the median. The box extends from the 25th to 75th percentiles. Whiskers represent minimum and maximum.

Extended Data

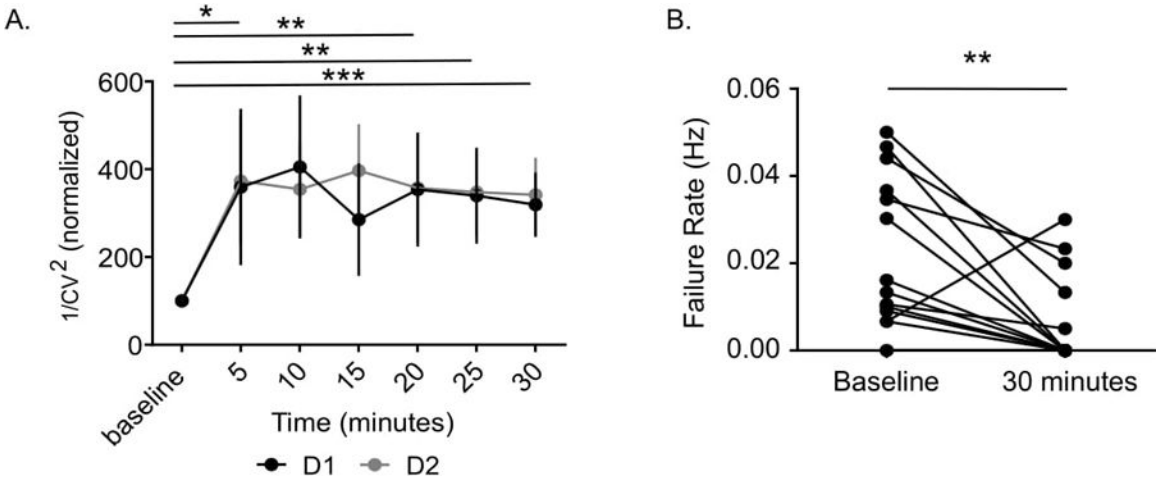

Extended Data Figure 1: High frequency stimulation also induces presynaptic changes and uncovering of silent synapses.

A. HFS alters coefficient of variation (Friedman test and Dunn's post hoc Q=19.95, p=0.0028, n=18 cells). Center values represent mean and error bars represent SEM. B. HFS stimulation decreases failure rate as revealed by (Two-tailed paired t-test: t=3.123, p=0.0066, n=17 cells). *** p<0.001, ** p<0.01, *p<0.05

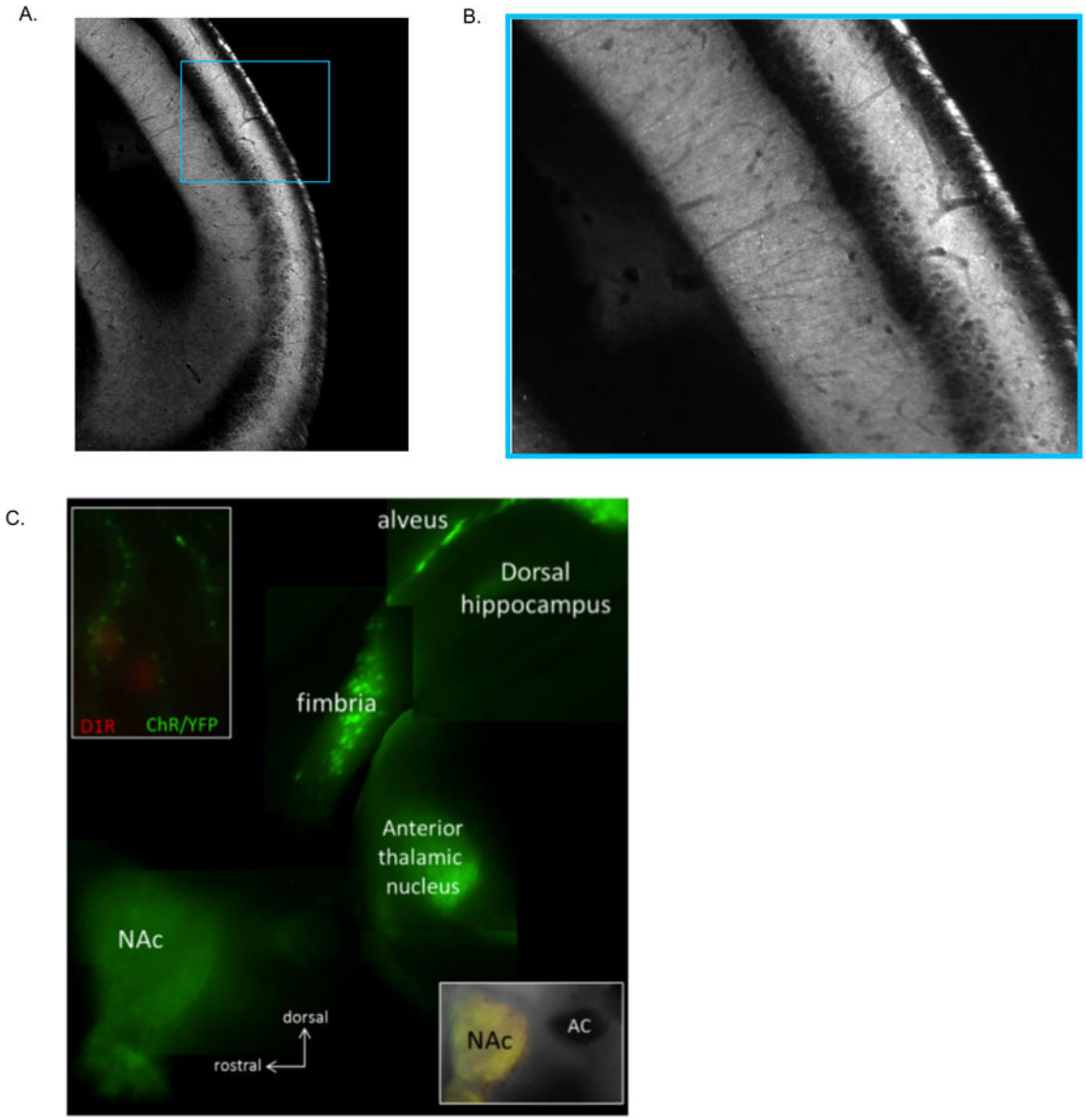

Extended Data Figure 2: Representative images of viral injection sites and expression

A. Low magnification image of YFP fluorescence in ventral hippocampus. B. Blue inset from A. C. Low magnification image showing YFP fluorescence in the NAc. Insets show overlap in labeling of D1R expression and YFP. This was repeated in mice used for optogenetic experiments. Scale bar indicates 100μM.

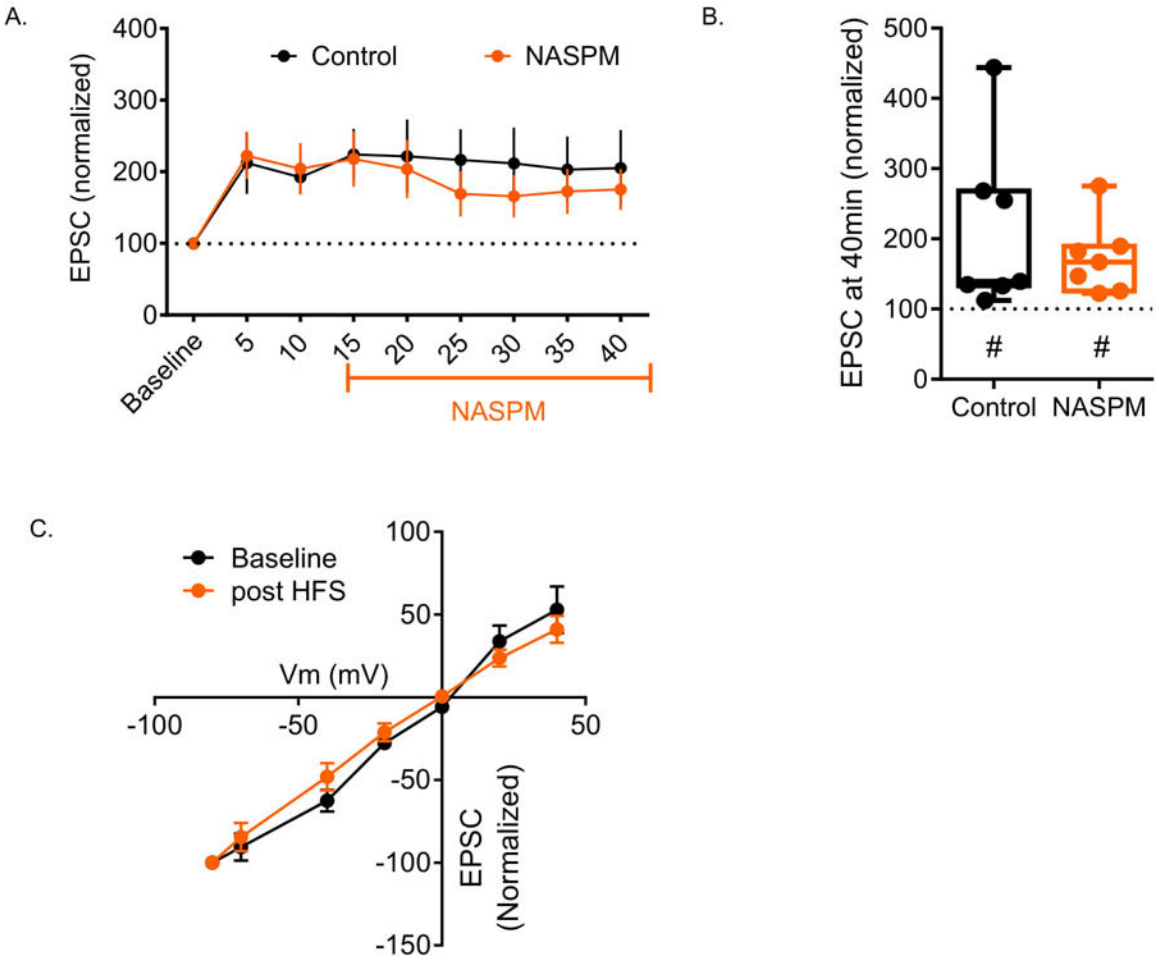

Extended Data Figure 3: LTP at hippocampus-NAc synapses is not associated with a preferential insertion of GluA2-lacking AMPA receptors

A. Wash-in of NASPM after LTP induction does not alter EPSC amplitude. Center values represent mean and error bars represent SEM. B: Summary data from the last five minutes of recording (Two-tailed Mann Whitney: U=24, p>0.9999, n=7,7 mice; Two-tailed paired t-test baseline EPSC amplitude/30 minutes post HFS: Control: t=2.508, p=0.046, n=7 cells; NASPM: t=2.747, p=0.0226, n=10 cells). C. HFS does not alter rectification at positive holding potentials (Two-tailed Mann Whitney: U=12, p=0.7879,n=7,4 mice). Center values represent mean and error bars represent SEM. # indicates significant increase in EPSC amplitude above baseline revealed by paired t-test. For box plots, the line in the middle of the box is plotted at the median. The box extends from the 25th to 75th percentiles. Whiskers represent minimum and maximum.

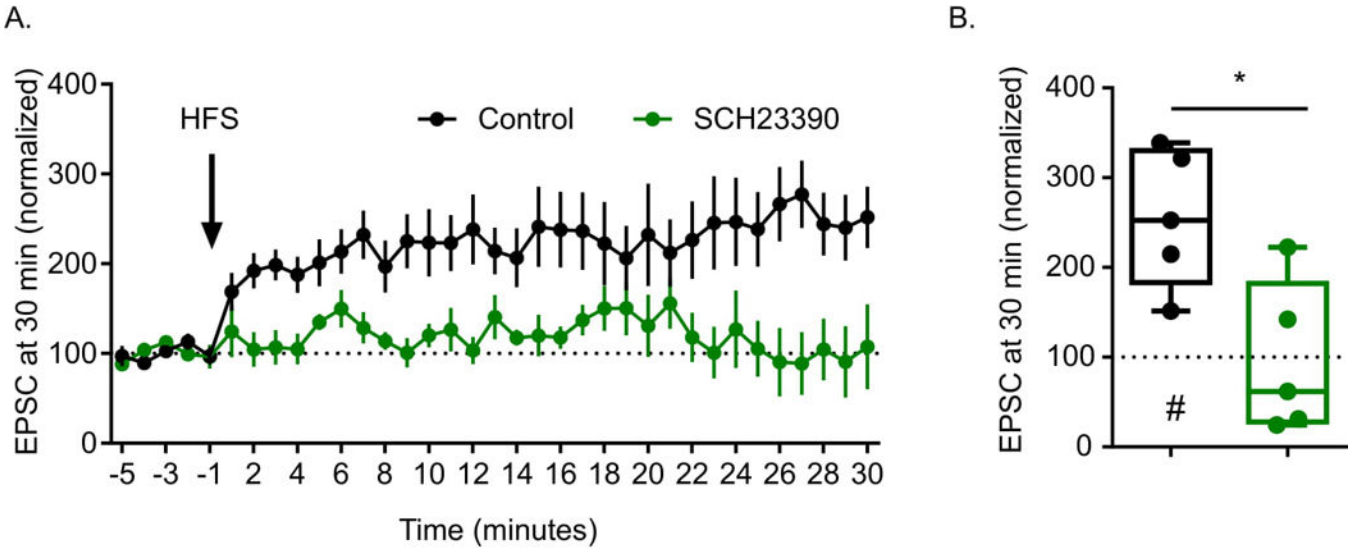

Extended Data Figure 4: D1 receptor signaling is required for LTP induction at non-specific NAc synapses.

A. Pre-incubation with D1 receptor antagonist SCH23390 blocks LTP induction in response to HFS. B. Summary data from the last 5 minutes of recording (Two-tailed Mann Whitney: U=2, p=0.0317, n=5 mice per group; #Two-tailed paired t-test baseline EPSC amplitude/30 minutes post HFS: Control: t=3.017, p=0.0393, n=5 cells; SCH: t=0.5016, p=0.6372, n=6 cells). LTP kinetic data are plotted in one minute bins. Center values represent mean and error bars represent SEM. For box plots, the line in the middle of the box is plotted at the median. The box extends from the 25th to 75th percentiles. Whiskers represent minimum and maximum.

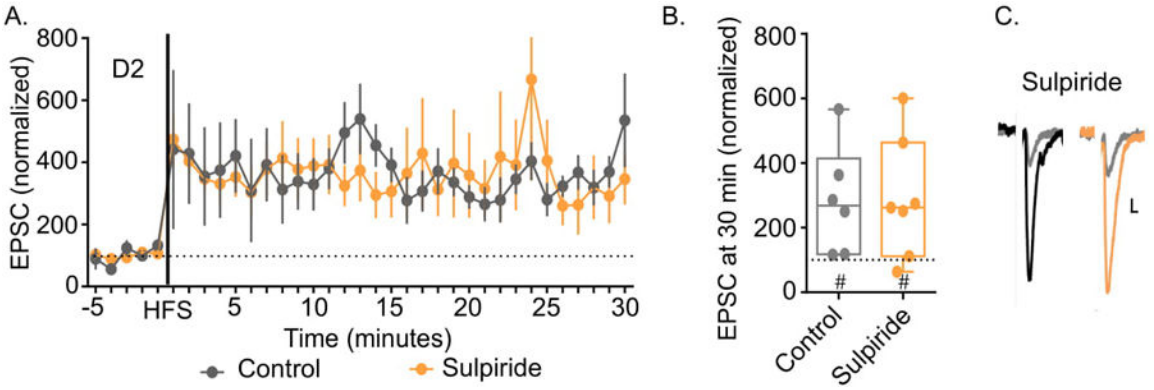

Extended Data Figure 5: D2 receptors are not required for LTP induction

A. Pre-incubation with D2-receptor antagonist sulpiride does not affect the ability to elicit LTP in response to HFS in D2RMSNs. B. Summary data from the last five minutes of recording (Two-tailed Mann Whitney: U=20, p=0.9452, n=6,7 mice #Two-tailed paired t-test baseline EPSC amplitude/30 minutes post HFS: Control: t=3.840, p=0.0121, n=6 cells; Sulpiride: t=4.246, p=0.0022, n=10 cells). C. Representative traces of EPSCs from control and sulpiride treated D2R-MSNs. # indicates significant increase in EPSC amplitude above baseline revealed by paired t-test. LTP kinetic data are plotted in one minute bins. Center

values represent mean and error bars represent SEM. For box plots, the line in the middle of the box is plotted at the median. The box extends from the 25th to 75th percentiles. Whiskers represent minimum and maximum. Scale bar for representative traces indicates 10pA/10ms.

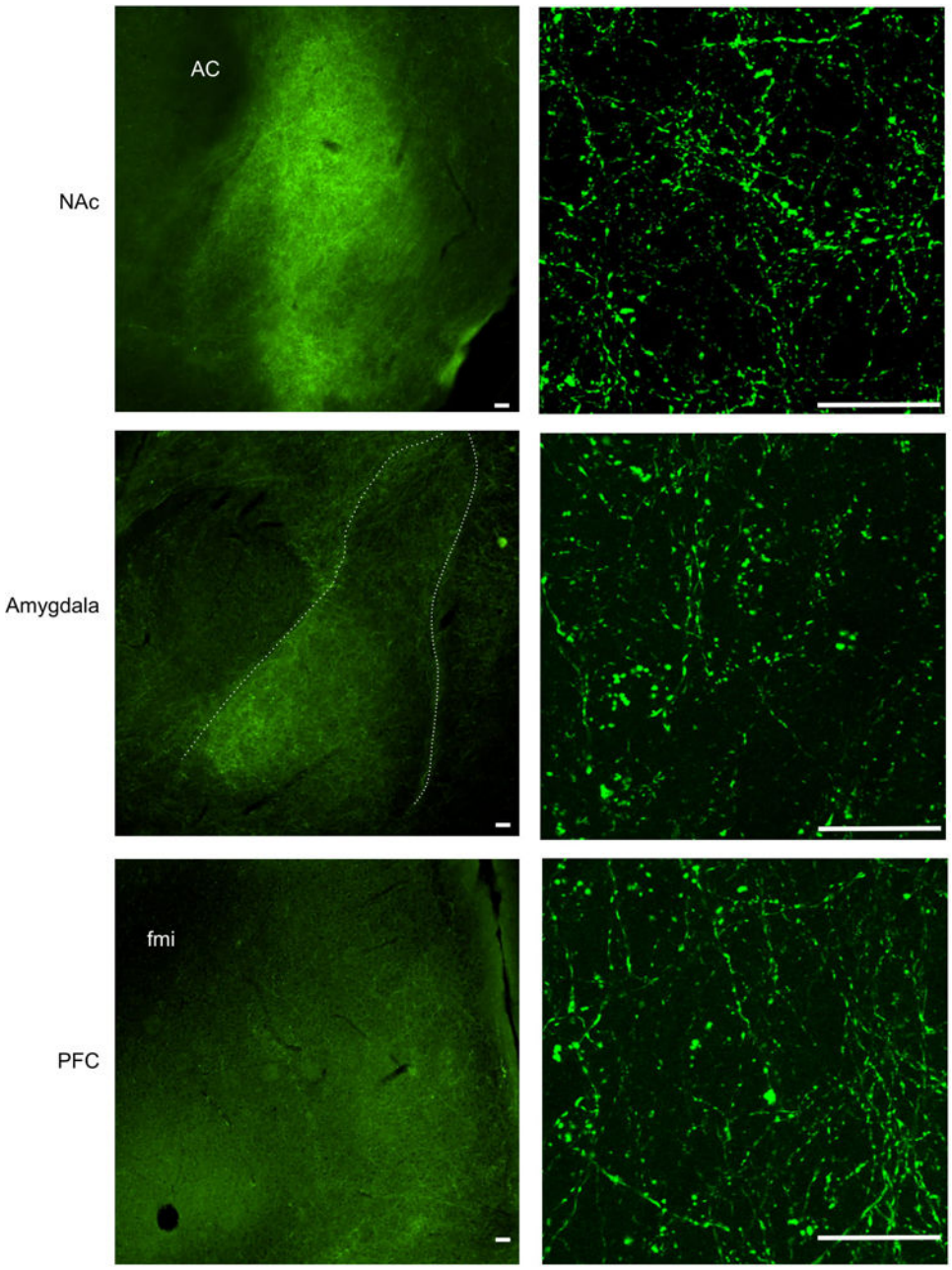

Extended Data Figure 6: Collaterals from hippocampus-NAc projecting cells

Representative images of labeled hippocampal fibers. Hippocampal cells projecting to the NAc were labeled by injecting a retrograde virus expressing Cre recombinase into the shell of the NAc and a Cre dependent virus containing YFP in the ventral hippocampus. Some collaterals are visible in the amygdala as well as the prelimibic and infralimbic regions of

the PFC. Right: 100× image showing labeling of fibers. Scalebars represent 50μm. AC represents anterior commissure. fmi represents the forceps minor of the corpus callosum. This was replicated in one other mouse.

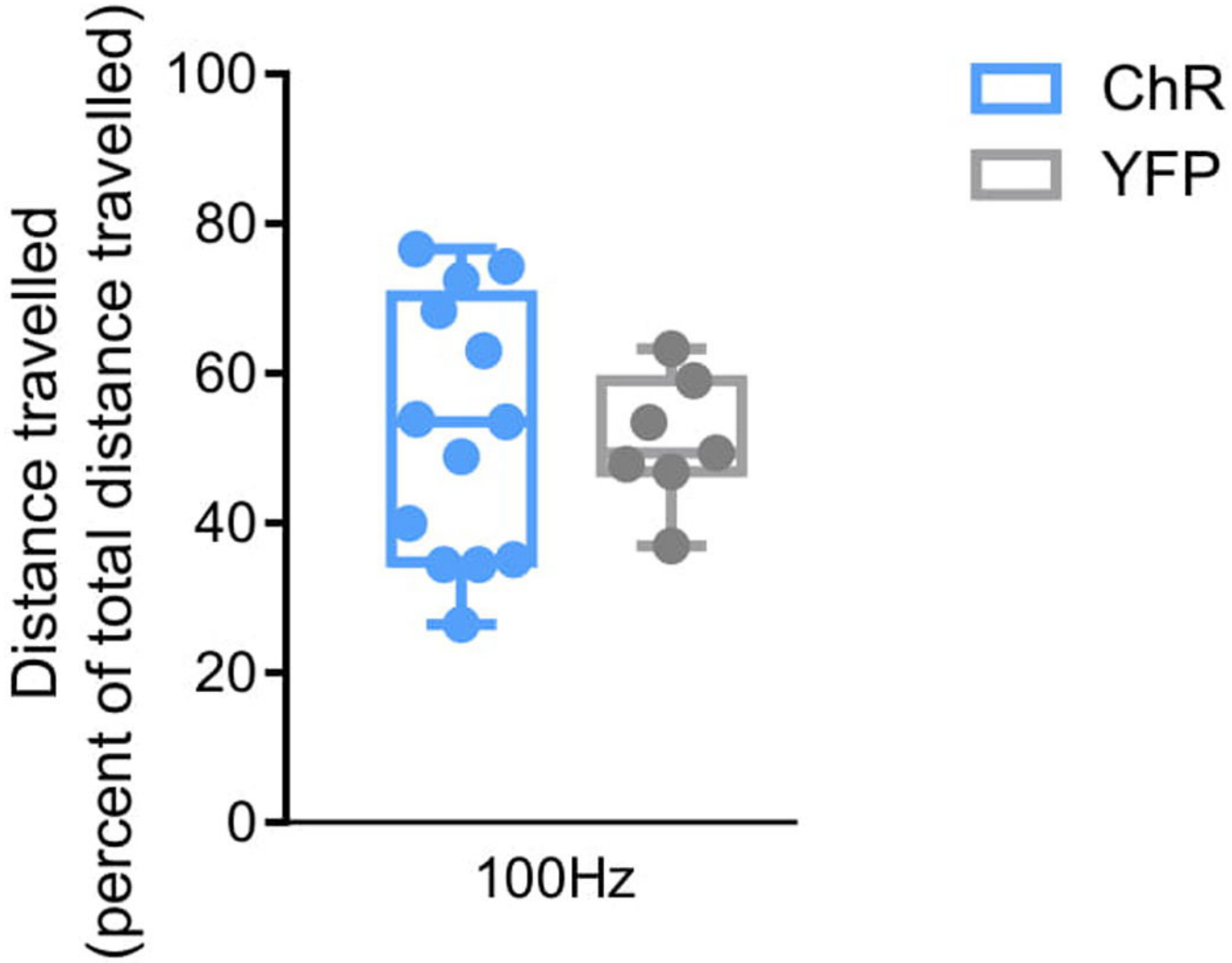

Extended Data Figure 7: High frequency stimulation does not alter locomotor activity

Distance travelled during the conditioning segment of the CPP paradigm. Data were normalized to the distance the mouse travelled during the 'no stimulation' portion of the test (Two-tailed Mann Whitney: U=43,p=0.8773, n=13,7 mice). The line in the middle of the box is plotted at the median. The box extends from the 25th to 75th percentiles. Whiskers represent minimum and maximum.

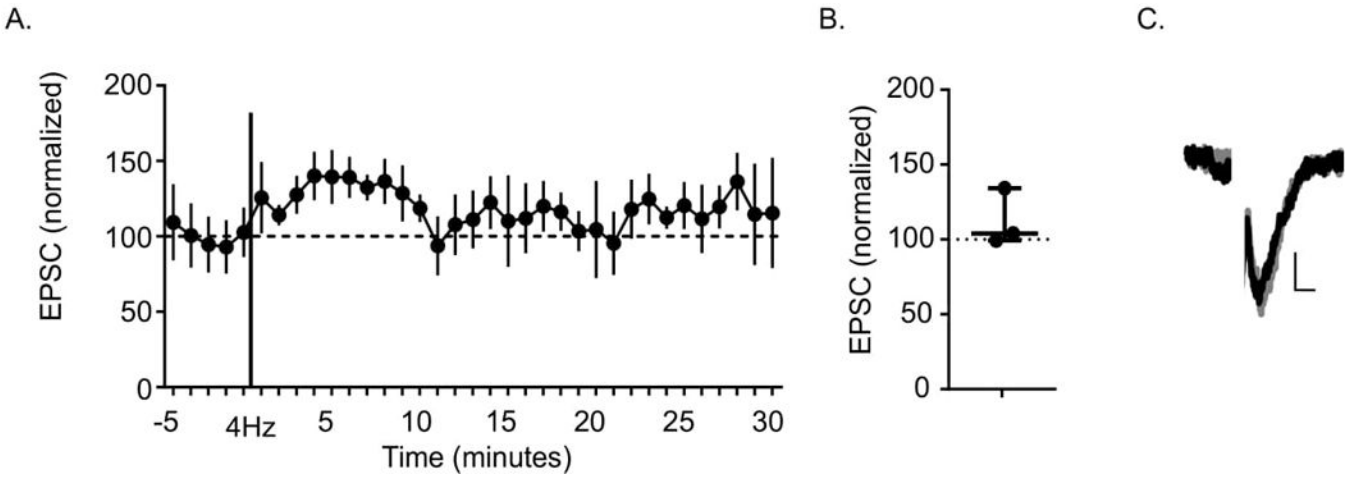

Extended Data Figure 8: 4Hz stimulation does not induce LTP

A. 4Hz stimulation does not potentiate EPSCs. Data are plotted in one minute bins. Center values represent mean and error bars represent SEM. B. Summary data from the last five minutes of recording (Two-tailed paired t-test: t=1.171 df=2, p= 0.3621, n=3 cells). The line in the middle of the box is plotted at the median. The box extends from the 25th to 75th percentiles. Whiskers represent minimum and maximum. Scale bar for representative traces indicates 10pA/10ms.

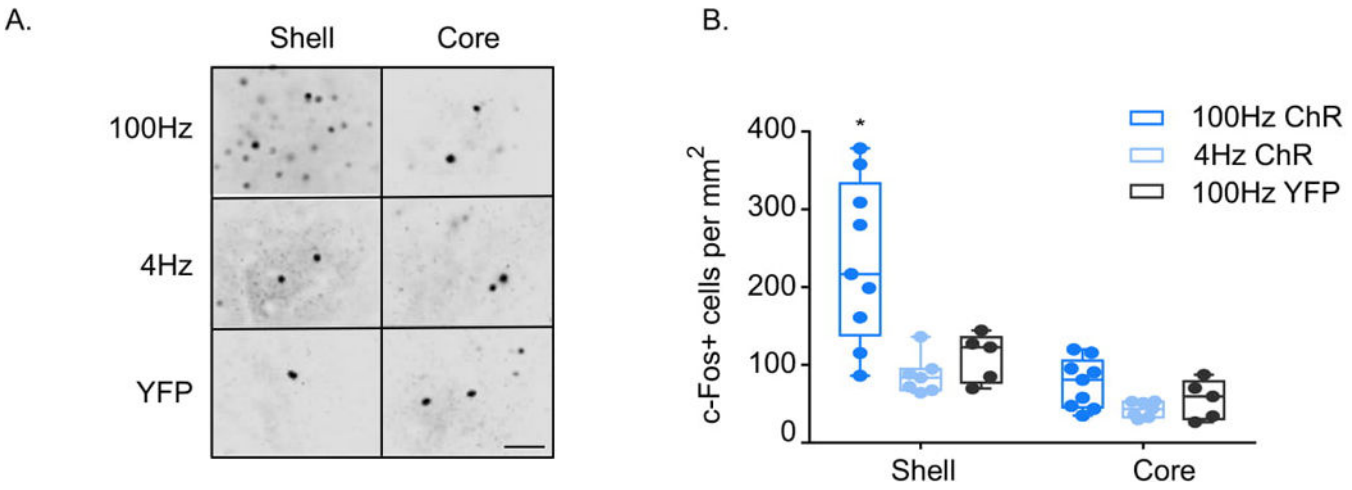

Extended Data Figure 9: High frequency stimulation induces c-Fos expression in the NAc shell

A. Representative images from NAc core and shell. Black/grey dots represent c-Fos positive cells. Scale bar indicates 50μm. B. 100Hz but not 4Hz stimulation increases c-Fos expression in the NAc shell (2-way ANOVA: $F_{(2, 36)} = 5.262$, p=0.0099, n=9,5,7 mice).

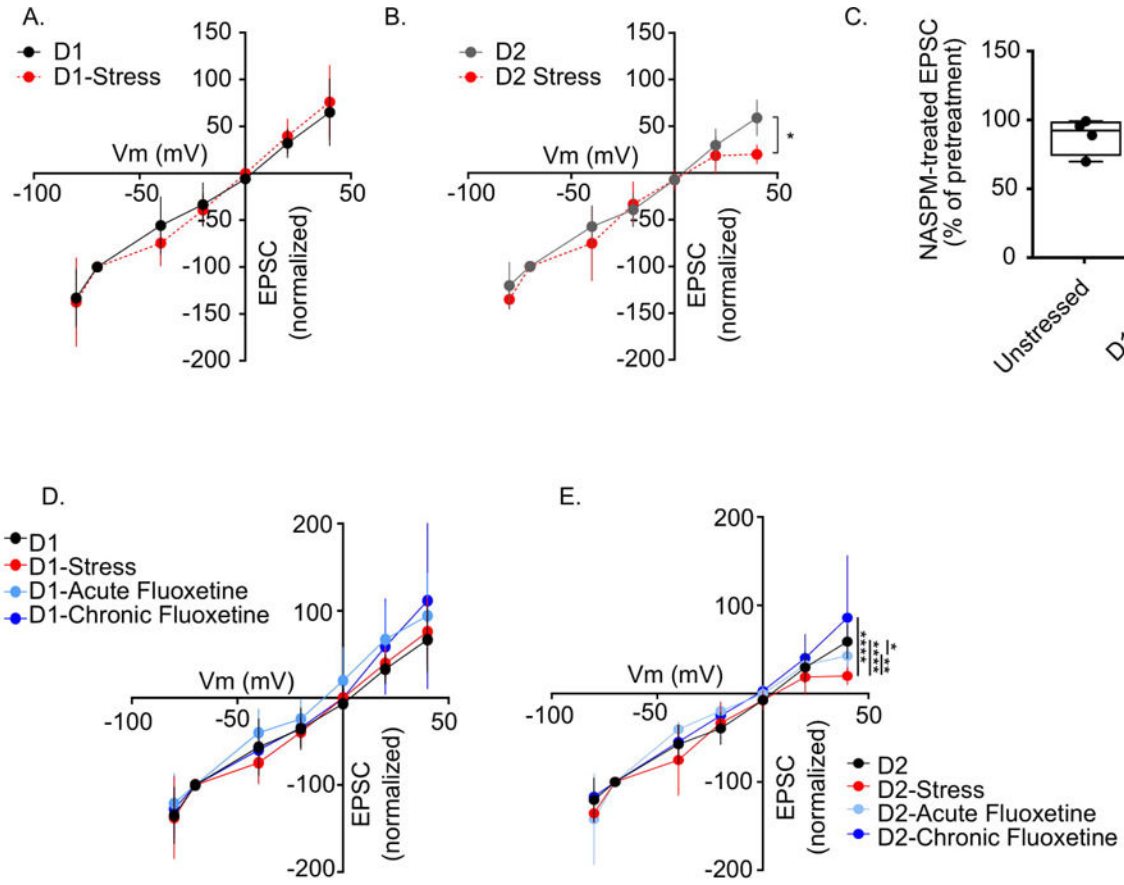

Extended Data Figure 10: Chronic stress leads to a preferential insertion of GluA2-lacking AMPA receptors in D2RMSNs.

A. Chronic stress does not alter subunit composition in D1R-MSNs (Two-tailed Mann Whitney of amplitude at +40mV: U=35, p=0.6665, n=6,7 mice). B. D2R-MSNs from mice exposed to chronic stress show inward rectification at positive membrane potentials (Two-tailed Mann Whitney of amplitude at +40mV: U=0, p=0.0006, n=6,7 mice C. NAPSM decreases EPSC amplitude in D2R-MSNs from mice exposed to chronic stress (Kruskal-Wallis test: H=7.423, p=0.0132, n=4 mice per group). D. Current/voltage relationships in D1R-MSNs remain unaffected by chronic stress or fluoxetine treatment (Kruskal-Wallis test with Dunn's post hoc: H=0.9436, p=0.8149, n=5,5,5,4 mice). E. D2R-MSNs from mice exposed to chronic stress treated with chronic fluoxetine show a linear current/voltage relationship, similar to unstressed controls. Inward rectification is observed in D2R-MSNs from mice exposed to chronic stress alone or chronic stress with acute fluoxetine treatment (Kruskal-Wallis test with Dunn's post hoc: H=31.42, p<0.0001, n=5,5,5,8 mice). The line in the middle of the box is plotted at the median. The box extends from the 25th to 75th percentiles. Whiskers represent minimum and maximum. Center values represent mean and error bars represent SEM. **** p<0.0001, ** p<0.01, *p<0.05.

Supplementary Material

Refer to Web version on PubMed Central for supplementary material.

Acknowledgements

We thank Dr. Brian Mathur for providing D1-tdtomato mice and Dr. Karl Deisseroth for permission to use the viral optogenetic constructs. We are grateful to the University of Maryland School of Medicine Center for Innovative Biomedical Resources, Confocal Microscopy Core for use of the confocal microscopes. We also thank Drs. Todd Gould, Tom Blanpied, and Tracy Bale for their suggestions and advice. This work was supported by R01MH086828 (SMT), T32 NS007375 (TAL), NARSAD Young Investigator Award (TAL), the Whitehall Foundation 2017–12-54 (MCC and JRT), and R01MH106500 (MKL and TCF).

References

1. Goto Y & O'Donnell P Synchronous activity in the hippocampus and nucleus accumbens in vivo. J. Neurosci. 21, 1–5 (2001).
2. O'Donnell P & Grace AA Synaptic interactions among excitatory afferents to nucleus accumbens neurons: hippocampal gating of prefrontal cortical input. J. Neurosci. 15, 3622–3639 (1995). [PubMed: 7751934]
3. Freyja Ólafsdóttir H, Barry C, Saleem AB, Hassabis D & Spiers HJ Hippocampal place cells construct reward related sequences through unexplored space. Elife 4, 1–17 (2015).
4. Tryon VL et al. Hippocampal neural activity reflects the economy of choices during goal-directed navigation. Hippocampus 27, 743–758 (2017). [PubMed: 28241404]
5. Gauthier JL & Tank DW A Dedicated Population for Reward Coding in the Hippocampus. Neuron 99, 179–193 (2018). [PubMed: 30008297]
6. Sjulson L, Peyrache A, Cumpelik A, Cassataro D & Buzsáki G Cocaine Place Conditioning Strengthens Location-Specific Hippocampal Coupling to the Nucleus Accumbens. Neuron 926–934 (2018). doi:10.1016/j.neuron.2018.04.015
7. Gerfen CR et al. D1 and D2 Dopamine Receptor-Regulated Gene Expression of Striatonigral and Striatopallidal Neurons Published by: American Association for the Advancement of Science Stable URL: http://www.jstor.org/stable/2878403 07-06-2016 11: 45 UTC Your u. Science (80-.). 250, 1429–1432 (1990). [PubMed: 2147780]
8. Nicoll RA & Malenka RC Contrasting properties of two forms of long-term potentiation in the hippocampus. Nature 377, 115–118 (1995). [PubMed: 7675078]
9. Terrier J, Lüscher C & Pascoli V Cell-Type Specific Insertion of GluA2-Lacking AMPARs with Cocaine Exposure Leading to Sensitization, Cue-Induced Seeking, and Incubation of Craving. Neuropsychopharmacology 41, 1779–1789 (2016). [PubMed: 26585289]
10. Mangiavacchi S & Wolf ME D1 dopamine receptor stimulation increases the rate of AMPA receptor insertion onto the surface of cultured nucleus accumbens neurons through a pathway dependent on protein kinase A. J. Neurochem. 88, 1261–1271 (2004). [PubMed: 15009682]
11. Pawlak V & Kerr JND Dopamine receptor activation is required for corticostriatal spike-timing-dependent plasticity. J. Neurosci. 28, 2435–2446 (2008). [PubMed: 18322089]
12. Azdad K et al. Dopamine D2 and adenosine A2A receptors regulate NMDA-mediated excitation in accumbens neurons through A2A-D2 receptor heteromerization. Neuropsychopharmacology 34, 972–986 (2009). [PubMed: 18800071]
13. Cahill E et al. D1R/GluN1 complexes in the striatum integrate dopamine and glutamate signalling to control synaptic plasticity and cocaine-induced responses. Mol. Psychiatry 19, 1295–1304 (2014). [PubMed: 25070539]
14. Schotanus SM & Chergui K Dopamine D1 receptors and group I metabotropic glutamate receptors contribute to the induction of long-term potentiation in the nucleus accumbens. Neuropharmacology 54, 837–844 (2008). [PubMed: 18272187]
15. Lim BK, Huang KW, Grueter B. a., Rothwell PE & Malenka RC Anhedonia requires MC4R-mediated synaptic adaptations in nucleus accumbens. Nature 487, 183–189 (2012). [PubMed: 22785313]
16. Thompson SM et al. An excitatory synapse hypothesis of depression. Trends Neurosci. 38, 279–294 (2015). [PubMed: 25887240]

17. Hikida T, Kimura K, Wada N, Funabiki K & Nakanishi Shigetada S Distinct Roles of Synaptic Transmission in Direct and Indirect Striatal Pathways to Reward and Aversive Behavior. Neuron 66, 896–907 (2010). [PubMed: 20620875]

18. Lobo MK et al. Cell type - Specific loss of BDNF signaling mimics optogenetic control of cocaine reward. Science (80-.). 330, 385–390 (2010).

19. Kravitz AV, Tye LD & Kreitzer AC Distinct roles for direct and indirect pathway striatal neurons in reinforcement. Nat. Neurosci. 15, 816–818 (2012). [PubMed: 22544310]

20. Pascoli V, Turiault M & Lüscher C Reversal of cocaine-evoked synaptic potentiation resets drug-induced adaptive behaviour. Nature 481, 71–5 (2012).

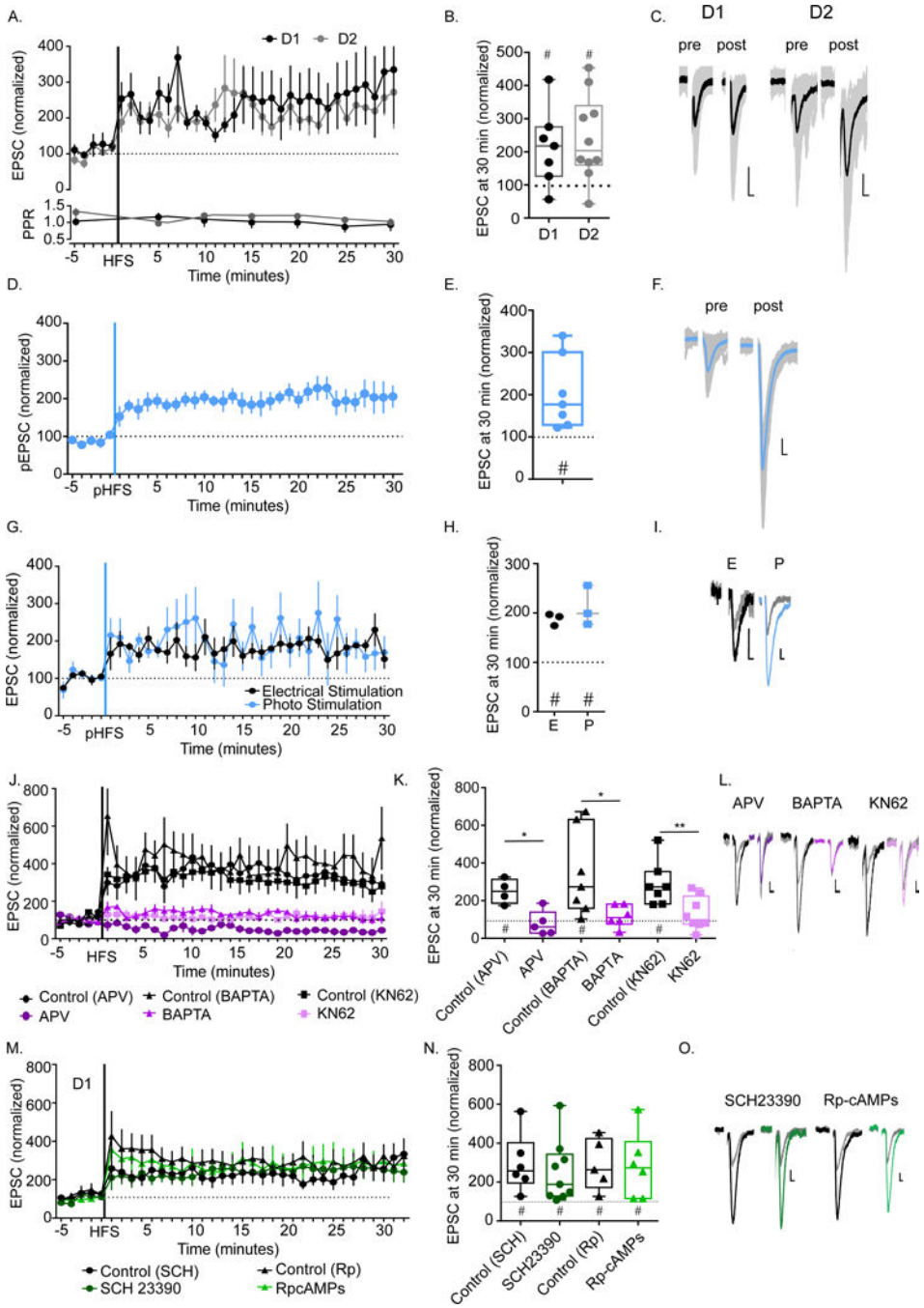

Figure 1: Mechanisms underlying activity-dependent long term potentiation at hippocampal-NAc synapses

A. LTP of hippocampal-NAc eEPSCs is similar in D1- and D2-MSNs and does not alter PPR. B. Summary data from the last five minutes of recording. (#D1:t=2.624, p=0.0394, n=7 cells from 7 mice; D2:t=3.586, p=0.0059, n=10 cells from 10 mice). C. Representative traces of EPSCs before/after HFS. Grey shading represents individual traces. Black represents the average. D. pHFS induces LTP of light-evoked EPSCs. E. Summary data from the last five minutes of recording. (# t=3.337,p=0.0157,n=7 cells/7 mice). F. Representative traces of pEPSCs before/after HFS. Grey shading represents individual traces. Blue represents the

average. G. pHFS potentiates both electrically- and optogenetically-evoked EPSCs. H. Summary data from the last five minutes of recording (#Two-tailed paired Wilcoxon to compare baseline to response at 30 minutes: W=21,p=0.0313,n=3 cells/3 mice). I. Representative traces from electrical- and optogenetically-evoked EPSCs before/after HFS. J. Pre-incubation with APV, KN62, or chelation of intracellular Ca2+ with BAPTA prevents LTP induction by HFS. K. Summary data from the last five minutes of recording (APV/ $Control_{APV}$: *U=1, p= 0.0317, n=3,5 mice # $Control_{APV}$: t=2.865,p=0.0457,n=5 cells; APV: t=1.729,p=0.1589,n=5 cells; BAPTA/$Control_{BAPTA}$: *U=5,p=0.0221,n=7,6 mice # $Control_{BAPTA}$: t=3.149,p=0.0199,n= 7 cells BAPTA: t=1.172,p=0.2942,n=6 cells; KN62/ $Control_{KN62}$: **U=6,p=0.0089,n=7,8 mice # $Control_{KN62}$: t=2.526,p=0.0449,n=7 cells KN62: t=0.4919,p=0.6378,n= 8 cells). L. Representative traces of EPSCs from control and APV, BAPTA, and KN62 treated cells. M. Pre-incubation with SCH 23390 or Rp-cAMPs does not affect LTP induction in D1R-MSNs. N. Summary data from the last five minutes of recording (SCH/$Control_{SCH}$: U=22,p=0.6070,n=6,9 mice # $Control_{SCH}$: t=5.658,p=0.0013,n=7 cells SCH: t=2.914,p=0.0195,n=9 cells; Rp/$Control_{Rp}$: U=13,p=0.7922,n=5,6 mice # $Control_{Rp}$: t=2.611,p=0.476,n=6 cells Rp: t=2.337,p=0.0476,n=9 cells). O. Representative traces of EPSCs from control, SCH23390, and Rp-cAMPs treated D1R-MSNs. *indicates differences between treatment and control as revealed by two-tailed Mann-Whitney U. # indicates significant increase in EPSC amplitude above baseline revealed by two-tailed paired t-test. LTP kinetics are plotted in one-minute bins. Center values represent mean and error bars represent SEM. For box plots, the middle line is plotted at the median. The box extends from 25^{th}-75^{th} percentiles. Whiskers represent minimum and maximum. Scale bar indicates 10pA/10ms.

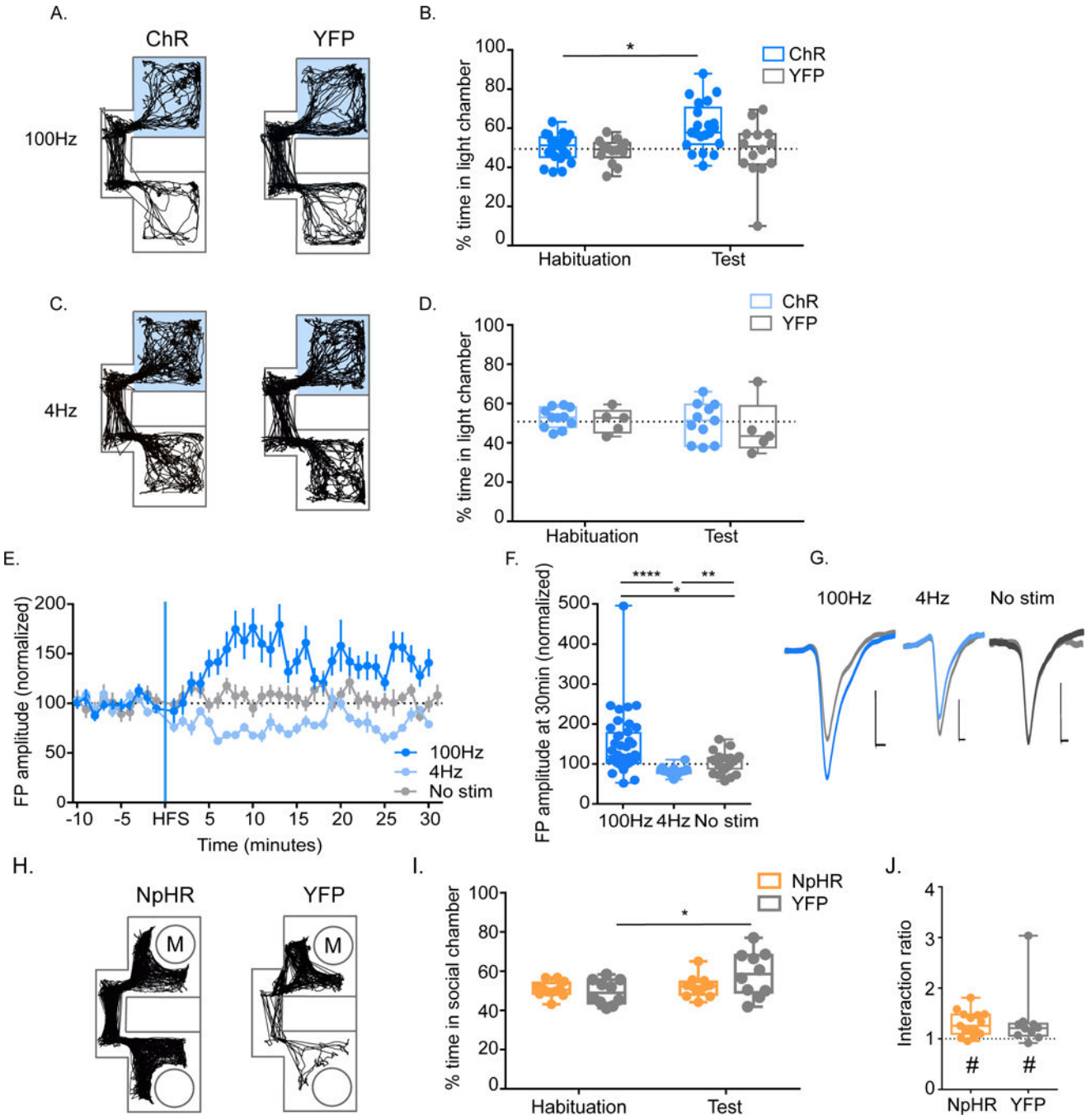

Figure 2: *In vivo* high frequency stimulation influences reward related behavior and NAc activity

A. Representative behavioral trace after 100Hz conditioning. B. Conditioning with 100Hz induces CPP in ChR-expressing mice (Two-way RM ANOVA with Sidak's post-hoc $F_{(1, 33)} = 5.155$,p=0.0298,n=21,14 mice). C. Representative behavioral trace after 4Hz conditioning. D. Conditioning with 4Hz light stimulation is not sufficient to induce CPP (Two-way RM ANOVA: $F_{(1, 14)} = 0.08221$,p=0.7785,n=11,5 mice). E. pHFS induces LTP of vHipp-NAc synapses *in vivo*. Data are plotted in one minute bins. Center values represent mean and error bars represent SEM. F. Summary data from the last five minutes of recording (Kruskal-

Wallis test with Dunn's multiple comparison post hoc: H= 34.58,p<0.0001,n=40, 24, 25 units from 4 mice). G. Representative traces of light-evoked LFPs. Scale bar represents 0.01mV/10ms. H. Representative behavioral trace after social interaction conditioning. M: location of the mouse during conditioning. I. vHipp-NAc silencing during conditioning blocks social interaction-induced CPP (Two-way RM ANOVA with Sidak's post-hoc: $F_{(1,20)}$=4.529,p=0.0459,n=12,10). J. vHipp-NAc silencing does not disrupt social interaction (Two-tailed Mann Whitney: U=64,p=0.5671,n= 15,10 mice). # One sample Wilcoxon shows significant interaction ratios for both groups (NpHR:W=114,p=0.0003,n=15 mice; YFP: W=49,p=0.0098,n=10 mice). For box plots, the middle line is plotted at the median. The box extends from 25th-75th percentiles. Whiskers represent minimum and maximum. **** p<0.0001, ** p<0.01, *p<0.05

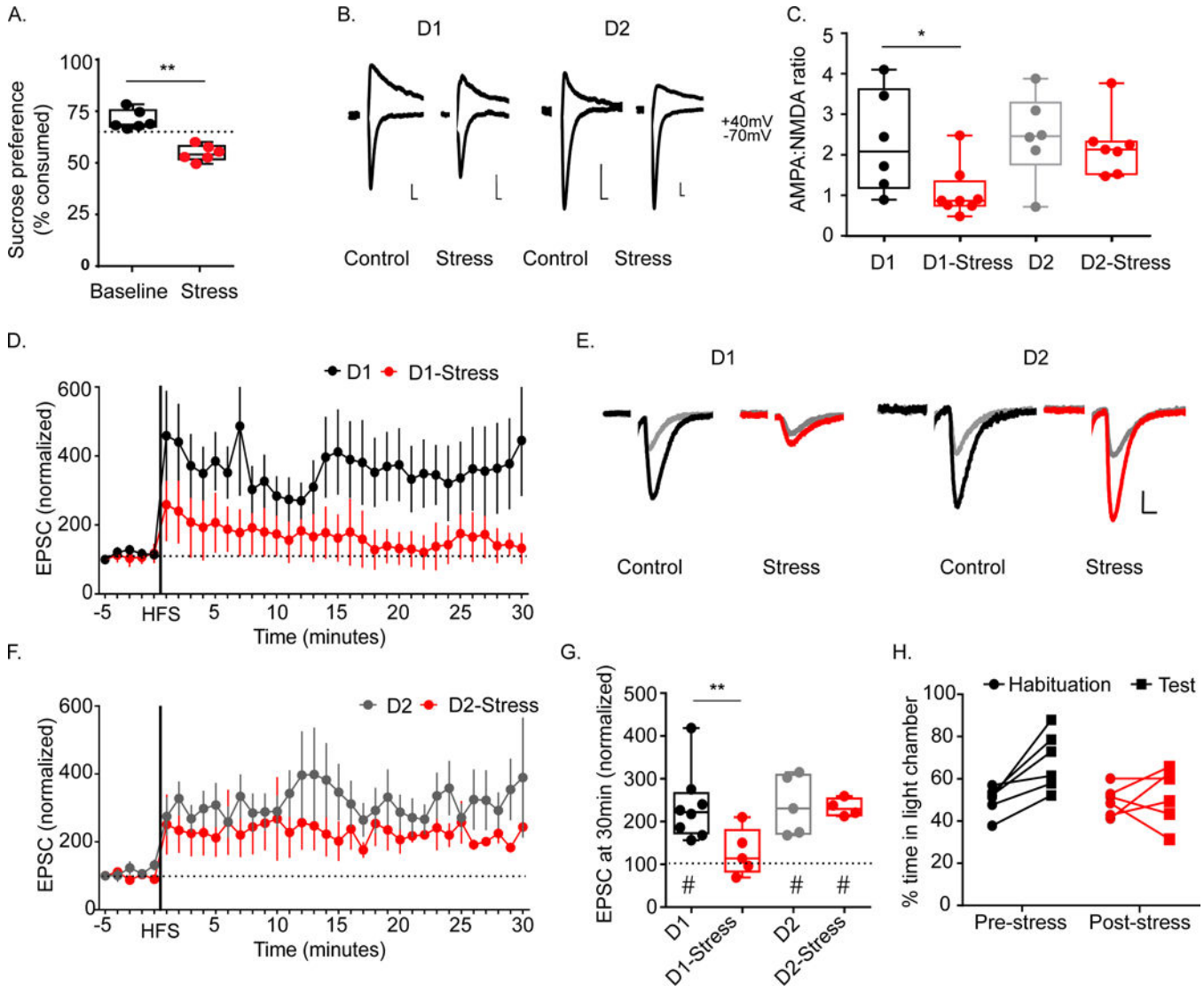

Figure 3: Chronic multimodal stress weakens excitatory hippocampal input onto D1R-MSNs.

A. Chronic stress induces loss of sucrose preference (Two-tailed paired t-test:t=5.056,p=0.0039,n=6 mice) Dotted line represents criteria for anhedonia. B. Representative traces of EPSCs at −70mV and +40mV from control mice and mice exposed to chronic stress. C. Chronic stress decreases AMPA:NMDA ratio (two-tailed t-test: t=2.422,p=0.0322,n=6,8 mice). D. D1R-MSNs from mice exposed to chronic stress show a deficit LTP induction. E. Representative traces of EPSCs mice exposed to chronic stress and controls. F. Chronic stress has no effect on LTP in D2R-MSNs. G. Summary data from the last five minutes of recording (*Two-tailed Mann Whitney: U=3, p=0.0109, n=8,5 mice; #Two-tailed paired t-test baseline EPSC amplitude/30 minutes post HFS: $D1_{Control}$:t=3.787, p=0.0068, n=8 cells; $D1_{Stress}$:t=1.222, p=0.2564, n=9 cells; $D2_{Control}$: t=3.854, p=0.012, n=6 cells; $D2_{Stress}$: t=3.164, p=0.0341, n=5 cells). H. Chronic stress abolishes pHFS-induced CPP (RM-ANOVA with Tukey post hoc: $F_{(2.109, 10.55)}$ = 5.551, p=0.0215, n= 6 mice). LTP kinetics are plotted in one-minute bins. Center values represent mean and error bars represent SEM. For box plots, the middle line is plotted at the median. The box extends from

25^{th}-75^{th} percentiles. Whiskers represent minimum and maximum. Scale bar indicates 10pA/10ms.

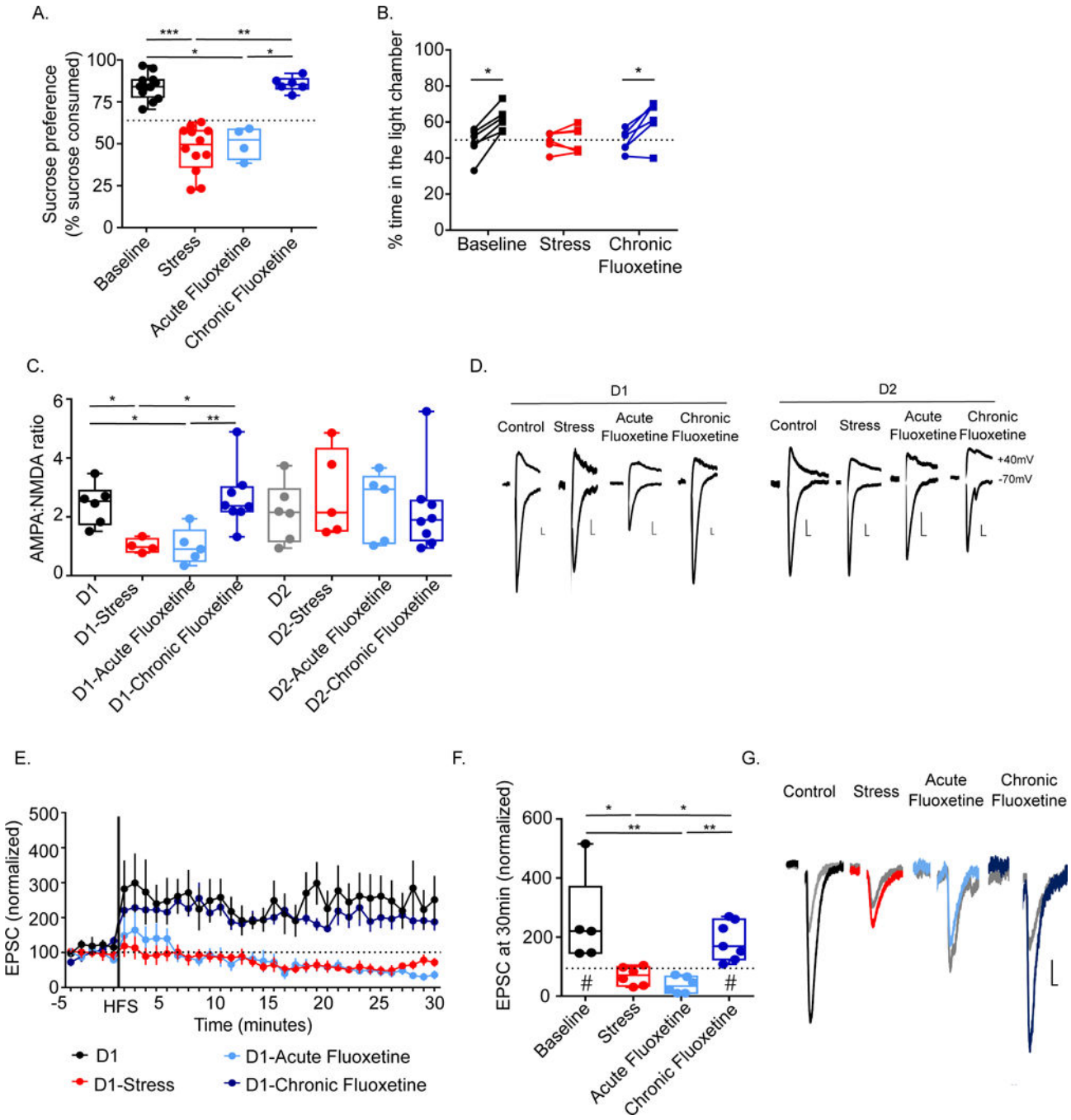

Figure 4: Antidepressant treatment rescues synaptic weakening induced by chronic stress

A. Chronic fluoxetine restores normal sucrose preference (One-way ANOVA Holm-Sidak's post-hoc F=36.38, p <0.0001, n=12,12,4,6 mice). Dotted line represents anhedonia criteria. B. Chronic fluoxetine restores CPP (Two-way RM ANOVA with Sidak's post-hoc $F_{(2,15)}$=7.293, p=0.0061, n=6 mice). C. Chronic fluoxetine restores stress-induced decrease in AMPA:NMDA ratio in D1-MSNs(ANOVA with Holm-Sidak's post-hoc D1: F=7.309, p= 0.0019, n=6,4,5,8 mice). D. Representative traces of EPSCs at −70mV and +40mV. E. Chronic fluoxetine restores LTP deficit induced by chronic stress. F. Summary data from the

last five minutes of recording (*Kruskal-Wallis test with Dunn's post-hoc: H=18.46,p= 0.0004,n=5,8,6,7 mice; #Two-tailed paired t-test baseline EPSC amplitude/30 minutes postHFS: $D1_{Control}$: t=4.540,p=0.0027,n=8 cells, $D1_{Stress}$: t=0.2615,p=0.8012,n=8 cells, $D1_{Acute}$:t=4.109,p=0.0093,n=6 cells, $D1_{Chronic}$: t=2.816,p=0.0305,n=7 cells). G. Representative traces of EPSCs before (grey) and after HFS (color). # indicates significant increase in EPSC amplitude above baseline revealed by paired t-test. LTP kinetics are plotted in one-minute bins. Center values represent mean and error bars represent SEM. For box plots, the middle line is plotted at the median. The box extends from 25^{th}-75^{th} percentiles. Whiskers represent minimum and maximum. *** p<0.001, ** p<0.01, *p<0.05 Scale bar indicates 10pA/10ms.